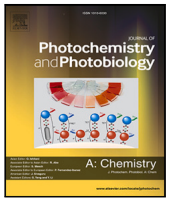
Journal of Photochemistry & Photobiology, A: Chemistry 452 (2024) 115589



Contents lists available at ScienceDirect

Journal of Photochemistry & Photobiology, A: Chemistry

journal homepage: www.elsevier.com/locate/jphotochem





Excited state dipole moments of two dicyanobenzene isomers from thermochromic shifts and *ab initio* calculations

Matthias Zajonz [a], Tim Oberkirch [a], Marie-Luise Hebestreit [a], Mirko Matthias Lindic [a], Christof Hättig [b], Michael Schmitt [a,*]

[a] Heinrich-Heine-Universität, Institut für Physikalische Chemie I, D-40225 Düsseldorf, Germany
[b] Ruhr-Universitaet Bochum, Lehrstuhl für Theoretische Chemie, D-44780 Bochum, Germany

ARTICLE INFO

Keywords:
1,2-Dicyanobenzene
1,3-Dicyanobenzene
Excited state
Dipole moment
Thermochromic shift
ab initio
COSMO

ABSTRACT

The excited state dipole moments of two positional isomers of dicyanobenzene have been determined from thermochromic shifts of the absorption and fluorescence emission spectra in ethyl acetate solution and compared to the results of *ab initio* calculations. We found that the dipole moments of excited states from thermochromic shifts closely resemble the *ab initio* values of the isolated molecule, while the results of conductor-like screening model (COSMO) using the same wave function model as for the isolated molecule, shows considerable deviations from the experimental values. It is shown that the dipole moments of the two cyano groups add up vectorially for both the ground and excited states.

1. Introduction

The concept of dipole moments as measure of charge density distributions in molecules has been successfully used in chemistry for over 100 years [1,2]. One key to this success story is that dipole moments in electronic ground states follow the laws for summation of vectors, which are directed along individual chemical bonds. This enables intuitive assessment of molecular dipoles from increment rules. While this procedure has entered basic chemistry textbooks [3,4] and works well in numerous cases, the situation for electronically excited states is far more complex. Dipole moments in electronically excited states provide a good hint to the electronic nature of the excited state. The excited states of aromatic molecules can be classified, using the nomenclature of Platt as L_a, L_b, B_a, and B_b states, depending on the position of the wave functions' nodal planes. The lowest two excited singlet states, L_a and L_b are degenerate in benzene, their degeneracy is lifted upon substitution. Depending on the substituent(s) and their relative position, they can be energetically close, making a straightforward assignment difficult. However, since their excited state dipole moments differ considerably, these can be used for an unequivocal assignments of the states.

Recently, several aromatic species bearing cyano groups, have been detected via radio astronomy in the interstellar medium, among them aromatics as benzonitrile (BN) [5], 1,2-dicyanobenzene, 1,3-dicyanobenzene [6] and 1- and 2-cyanonaphthalene [7].

Electronic Stark spectroscopy of benzonitrile (BN), performed in the group of Pratt yielded the dipole moments in the ground and first excited singlet state [8]. Since their ground state dipole moment differs considerably from a value of 4.14(5) D, which was determined by microwave Stark spectroscopy [9], Wohlfart et al. used Fourier transform microwave spectroscopy in a supersonic jet, to determine the dipole moment of benzonitrile precisely. They found a value of μ_a = 4.5152(68) D, in good agreement with the value determined by Borst et al. of 4.48(1), which settled the dispute about the dipole moment of benzonitrile.

Sato-Toshima et al. determined the ground state dipole moments of 1,2-dicyanobenzene (12-DCB) and 1,3-dicyanobenzene (13-DCB) in benzene and dioxan solutions using the method of Guggenheim [10]. Chitarra et al. measured the rotational spectra of 12-DCB and 13-DCB in the centimeter- and millimeter-wave domains and determined their ground state rotational constants, the quartic and sextic centrifugal constants and the nuclear quadrupole coupling constants [6].

In the present contribution we will show, how the dipole moments of the cyano groups sum up vectorially in the two dicyanobenzenes for both the ground and the electronically excited states. Since both molecules have C_{2v} symmetry in both states, the direction of the dipole moment does not change upon excitation, just the modulus, which makes them ideal candidates for determination of their excited state dipoles *via* thermochromic shifts of their absorption and emission spectra in solution.

* Corresponding author.
E-mail address: mschmitt@hhu.de (M. Schmitt).

https://doi.org/10.1016/j.jphotochem.2024.115589
Received 28 December 2023; Received in revised form 27 February 2024; Accepted 10 March 2024
Available online 13 March 2024
1010-6030/© 2024 The Author(s). Published by Elsevier B.V. This is an open access article under the CC BY license (http://creativecommons.org/licenses/by/4.0/).

Table 1
SCS-CC2/cc-pVTZ calculated rotational constants A, B, C and inertial defects in the ground state (doubly primed values) and the excited state (primed values) of BN, 12-DCB, and 13-DCB. The inertial defect ΔI is defined as: $\Delta I = I_c - I_b - I_a$, where the I_g are the moments of inertia with respect to the main inertial axes $g = a, b, c$.

	BN		12-DCB		13-DCB	
	Calc.	Exp.[8]	Calc.	Exp.[6]	Calc.	Exp.[6]
A''/MHz	5656	5656.7(1)	2004	2000.710452(98)	2705	2723.018609(46)
B''/MHz	1535	1547.4(1)	1335	1346.325041(27)	899	906.419893(21)
C''/MHz	1208	1214.8(1)	801	804.503123(25)	675	679.859840(15)
$\Delta I''$/amuÅ^2	0.00	0.07(5)	0.00	0.211(1)	0.00	0.207(1)
A'/MHz	5470	5474.7(1)	1937	–	2633	–
B'/MHz	1495	1510.2(1)	1310	–	886	–
C'/MHz	1174	1183.9(1)	781	–	663	–
$\Delta I'$/amuÅ^2	0.00	0.08(6)	0.00	–	0.00	–
$\Delta A'$/MHz	−186	−182.0(1)	−68	–	−72	–
$\Delta B'$/MHz	−40	−37.2(1)	−25	–	−13	–
$\Delta C'$/MHz	−34	−30.9(1)	−20	–	−12	–

2. Computational methods

2.1. Quantum chemical calculations

Structure optimizations were performed with Turbomole, version 7.5.1 [11] employing a Dunning's correlation-consistent polarized valence triple zeta (cc-pVTZ) basis set from the Turbomole library [12,13]. The equilibrium geometries of the electronic ground and the lowest excited singlet states were optimized using the approximate coupled cluster singles and doubles model (CC2) employing the resolution-of-the-identity (RI) approximation [14–16]. For the structure optimizations spin-component scaling (SCS) modifications to CC2 were taken into account [17]. Additionally, ground state properties have been calculated at the RI-MP2 level of theory [18] for the isolated molecules and compared to those from the Conductor-like Screening Model (COSMO) [19]. Similarly, for the excited states gas phase values from the ADC(2) method [20] are compared to the respective solvation values from COSMO. Vibrational frequencies and zero-point corrections to the adiabatic excitation energies were obtained from numerical second derivatives using the NumForce script [21].

3. Experimental methods

The cavity volumes of the cyanoindoles and benzonitrile, dissolved in ethyl acetate were determined using a high-precision density meter from Anton Paar (model: DMA 4500). For this purpose, a concentration series was prepared and measured in a temperature range from 265.15 to 343.15 K with an increment of 2 K. The spectroscopic measurements were carried out in a self-constructed cell using two spectrometers from Varian. A Varian Cary 50 Scan UV–Visible was used for absorption measurements and a Cary Eclipse Fluorescence for emission measurements. The measurements were performed between 225.15 K and 343.15 K with an increment of 2 K. For the determination of the refractive indices of the solvent, a refractometer from Anton Paar (model: Abbemat MW) was used, whereby measurements were made on a temperature scale from 283.15 K to 343.15 K with an increment of 1 K. At each temperature refractive indices were determined at 5 different wavelengths. The permittivity of the solvent was determined using a Keysight E4990 A Impedance Analyzer in combination with the capacitor of a Keysight 16452 A Test Fixture.

4. Results and discussion

4.1. Computational results

The structures of BN, 12-DCB, and 13-DCB in the ground and the lowest two excited singlet states have been optimized at the SCS-CC2/cc-pVTZ level of theory, using the Turbomole program suite [11]. The ground state geometries are shown in Fig. 1. All Cartesian coordinates of the optimized structures are given in the online supporting material. The calculated rotational constants and inertial defects of the lowest two singlet states and dipole moment components on the main inertial axes for each molecule are presented in Table 1. The calculated inertial defects in the ground state of the three molecules are small and numerical artefacts of a planar structure. All three molecules possess C2v-symmetry in the electronic ground state, with the C_2-axis being the inertial a-axis for BN and 12-DCB and the b-axis for 13-DCB. The dipole moments are consequently oriented along the a-axis for BN and 12-DCB and along the b-axis for 13-DCB, cf. Fig. 1. The symmetry is preserved in the excited state, thus the orientation of the permanent dipole moment stays like in the ground state and only the modulus changes upon electronic excitation.

In order to compute dipole moments in solution, the conductor-like screening model (COSMO) [19] was used. Since COSMO for RI-CC2 calculations of the excited states is not implemented, we switched the dipole moment computations to (RI-)ADC(2) for the excited states and to (RI-)MP2 for the ground state. At first, we compared the dipole moments from the respective CC2 calculations to those from MP2 (S_0) and ADC(2) (S_1 and S_2). This comparison is shown in Table 3. Very close agreement shows, that the values from ADC(2) can indeed be used for the excited states in the COSMO model.

Adiabatic excitation energies and transition dipole moment orientation of the lowest two excited states of BN, 12-DCB, and 13-DCB have been calculated, including zero-point-energy correction at the level of optimization. These results are presented in Table 2 along with the vertical absorption and emission energies to and from the respective states. In all cases, the S_1-state, which is of $\pi\pi^*$ nature, is the L_b state ($^1B_2$) in Platt's notation [22], while the S_2-state can be described as L_a-state ($^1A_1$). The respective frontier orbitals are shown in Fig. 2. For BN, the transition dipole moment (TDM) of the S_1-state is oriented along the inertial b-axis, as has been confirmed experimentally and thus runs through the **b**onds, while that of the S_2-state is oriented along the inertial a-axis and runs through the **a**toms in agreement with Platt's L_a-L_b notation. The S_1 TDM of 12-DCB is oriented along the a-axis and runs though the bonds (L_b), while that of the S_2-state is parallel to the b-axis and runs through the atoms (L_a). For 13-DCB the S_1-TDM is again along the a-axis, running through the bonds and the S_1-TDM along b, running through the atoms. Mind the fact, that the molecules in Fig. 1 are oriented in such a way, that the C_2-symmetry axis and the permanent dipole moment vector are pointing upwards, which causes the inertial axes a and b to switch in 13-DCB compared to BN and 12-DCB.

4.2. Experimental results

First, the cavity volume of 12-DCB and 13-DCB in ethylacetate (EA), which is used to replace the Onsager radius [23,24] has been

Table 2
Adiabatic excitation energies $\tilde{\nu}_{ad.}$, vertical excitation energies $\tilde{\nu}^{exc.}_{vert.}$, vertical emission energies $\tilde{\nu}^{em.}_{vert.}$, and transition dipole moment orientation θ of the lowest two excited singlet states of BN, 12-DCB, and 13-DCB. θ is defined as the angle between the TDM and the inertial a-axis.

	BN		12-DCB		13-DCB	
	S_1	S_2	S_1	S_2	S_1	S_2
$\tilde{\nu}_{ad.}/cm^{-1}$	37 162	43 347	35 835	42 798	35 958	44 142
$\tilde{\nu}^{exc.}_{vert.}/cm^{-1}$	40 802	49 166	38 982	46 081	39 272	47 640
$\tilde{\nu}^{em.}_{vert.}/cm^{-1}$	36 755	43 912	35 228	34 307	35 464	36 029
$\theta/°$	90	0	0	90	0	90
LUMO ← HOMO	t'-	0.95	–	0.94	–	0.97
LUMO ← HOMO-1	0.75	–	0.75	–	0.72	–
LUMO+1 ← HOMO	0.63	–	−0.62	–	0.65	–

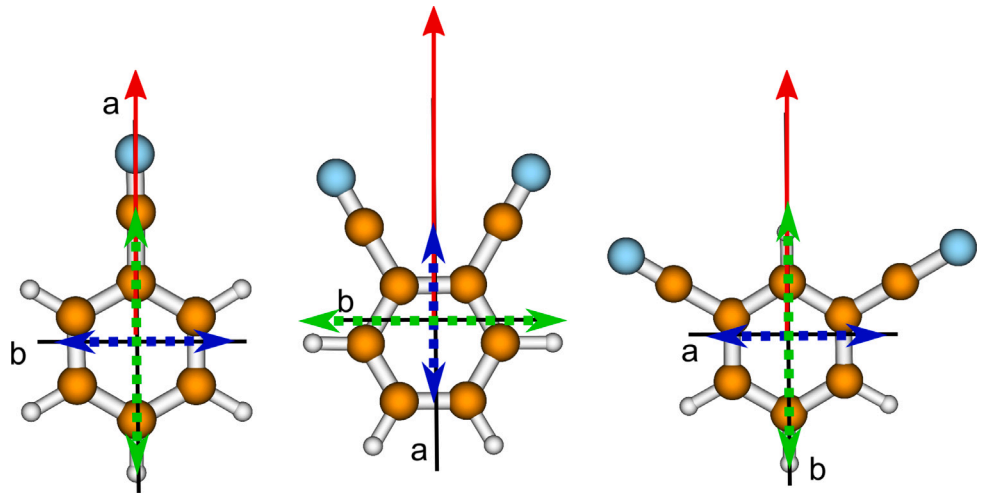


Fig. 1. SCS-CC2/cc-pVTZ optimized ground state geometries of benzonitrile, 12-DCB, and 13-DCB along with inertial axes a and b, the permanent dipole moment vector (red straight arrow), the transition dipole moment to the S_1-state (blue dotted double arrow), and the TDM to the S_2-state (green dotted double arrow).

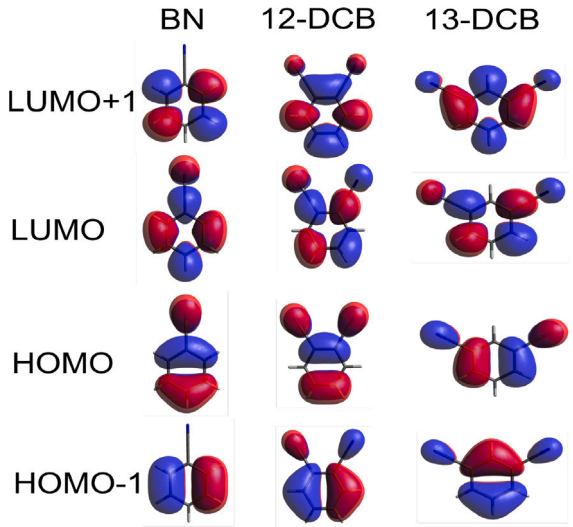


Fig. 2. Frontier orbitals of BN, 12-DCB, and 13-DCB. Orientation as in Fig. 1.

determined from the relation between the weight fraction w and the molar cavity volume V_m:

$$\frac{1}{\rho} = \frac{1}{\rho^*} + \left(\frac{V_m}{M} - \frac{1}{\rho^*}\right) \cdot w \tag{1}$$

where ρ is the density of the solution, ρ^* is the density of the solvent, V_m is the molar cavity volume, and M is the molar mass of the solute.

According to Eq. (1) the molar cavity volume can be calculated from the slope of a linear fit of the plot of the inverse density $\frac{1}{\rho}$ versus the weight fraction w at a given temperature. The fit at a temperature of 273 K is shown in Fig. 3. This procedure was repeated for each temperature, which was used for the determination of the thermochromic shifts, and the results were combined in Fig. 4.

The absorption and fluorescence maxima shift upon changing the solvent index of refraction and permittivity, what can be introduced by a variation of the solvent (solvatochromic shifts). Since both index of refraction and permittivity are functions of the temperature this shift can also be induced by a temperature variation (thermochromic shifts).

The shift of the fluorescence and absorption spectra of 12-DCB (a) and 13-DCB (b) with varying temperature is shown in Fig. 5. The lower red curve represent the lowest, the upper green curve the highest temperature in the series. The fluorescence maxima for both conformers shift red, to lower wavenumbers. Absorption maxima have a much smaller shift to the blue for 12-DCB and to the red for 13-DCB.

Lippert and Mataga derived an equation for evaluating the change of the dipole moment from solvatochromic shifts in different solutions [25,26]:

$$\tilde{\nu}_A - \tilde{\nu}_F = -\frac{2(\mu_e - \mu_g)^2}{4\pi\varepsilon_0 hca^3} \cdot F_{LM} + const. \tag{2}$$

where $\tilde{\nu}_A$ and $\tilde{\nu}_F$ are the wavenumbers of the maxima in absorption and fluorescence spectra, μ_g and μ_e are the ground and excited state dipole moment ε_0 is the vacuum permittivity, h the Planck constant, c the speed of light, a the Onsager cavity radius, and F_{LM} the solvent polarity function according to Lippert and Mataga:

$$F_{LM} = \frac{\varepsilon - 1}{2\varepsilon + 1} - \frac{n^2 - 1}{2n^2 + 1} \tag{3}$$

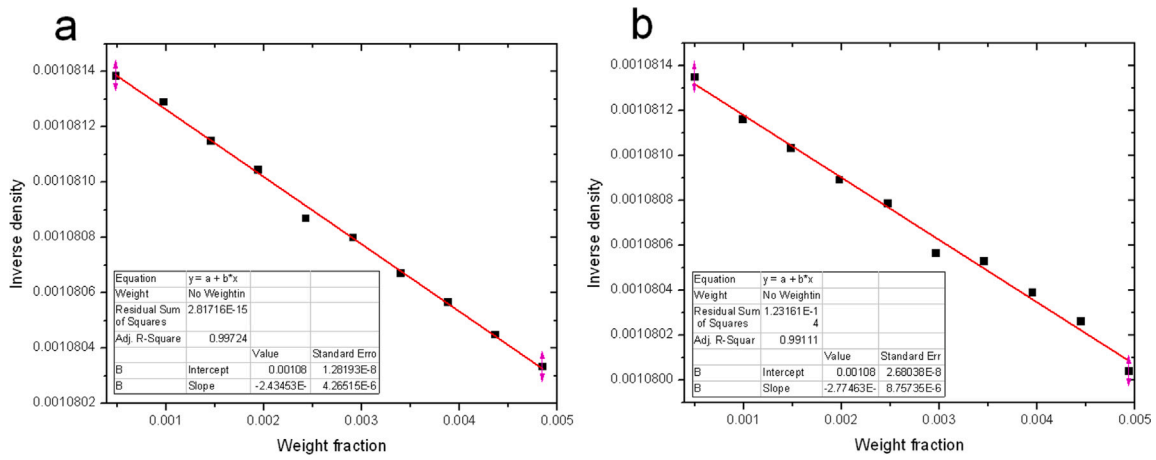


Fig. 3. Dependence of the inverse density of the 12-DCB solution in EA (a) and of 13-DCB (b) from the weight fraction.

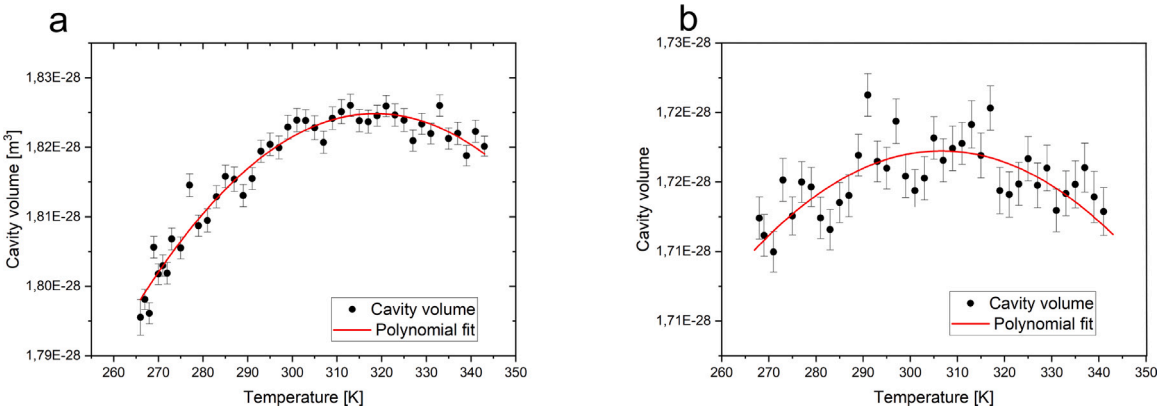


Fig. 4. Dependence of the cavity volume of 12-DCB (a) and 13-DCB (b) in EA from the temperature of the solution.

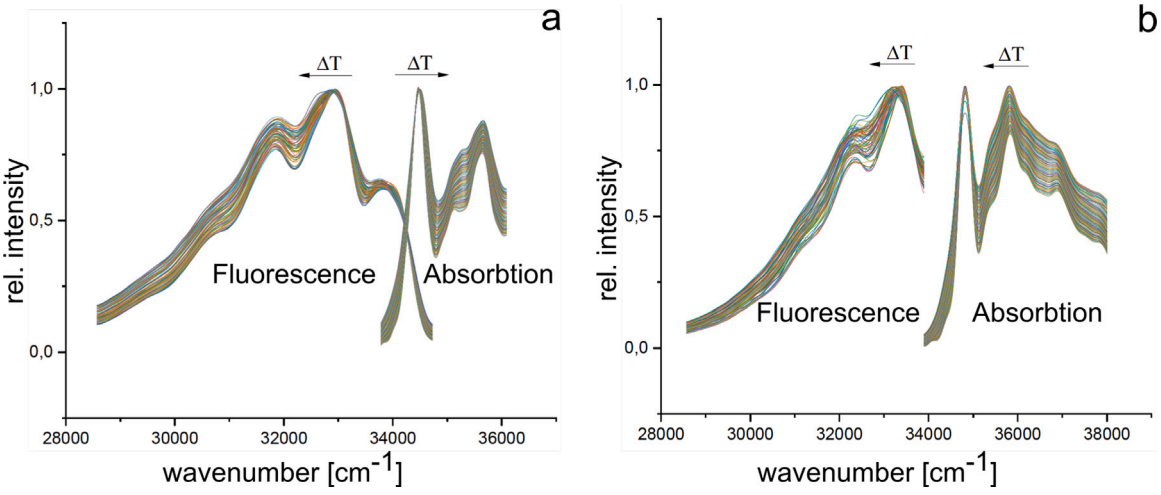


Fig. 5. Shift of the fluorescence and absorption spectra of 12-DCB (a) and 13-DCB (b) with varying temperature.

Using the experimentally determined cavity volume instead of the Onsager radius of the cavity, Eq. (2) becomes:

$$\tilde{\nu}_A(T) - \tilde{\nu}_F(T) = -\frac{2\left(\mu_e - \mu_g\right)^2}{3\varepsilon_0 hc} \cdot F_{LM}(T) + const. \quad (4)$$

$$F_{LM}(T) = \frac{1}{V(T)} \cdot \left[\frac{\varepsilon(T) - 1}{2\varepsilon(T) + 1} - \frac{n(T)^2 - 1}{2n(T)^2 + 1}\right] \quad (5)$$

The plot of $\tilde{\nu}_A(T) - \tilde{\nu}_F(T)$ (Eq. (4)) versus F_{LM} (5) yields the change of the dipole moment upon electronic excitation from the slope m_{LM} (see Fig. 6).

The second approach we will use here, has been introduced by Bilot and Kawski [27]. According to Bilot–Kawski a plot of the sum of fluorescence and absorption maxima vs. the solvent polarity function

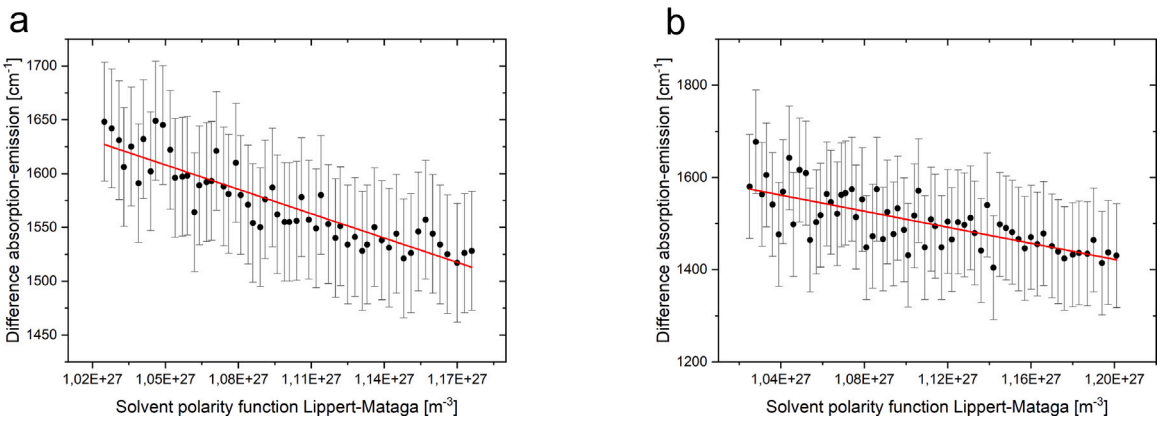


Fig. 6. Plot of $\tilde{\nu}_A(T) - \tilde{\nu}_F(T)$ versus F_{LM} for solutions of 12-DCB (a) and 13-DCB (b) in EA.

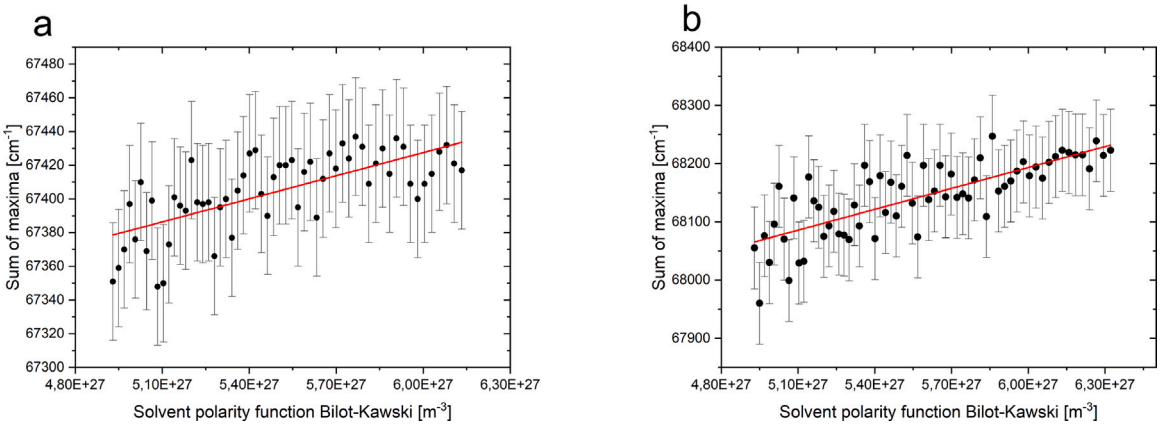


Fig. 7. Plot of $(\tilde{\nu}_A + \tilde{\nu}_F)$ versus $F_{BK}(T)$ for solutions of 12-DCB (a) and 13-DCB (b) in EA.

yield the excited state dipole moment, given that the ground state dipole is known:

$$\tilde{\nu}_A(T) + \tilde{\nu}_F(T) = -\frac{2\left(\mu_e^2 - \mu_g^2\right)}{3\epsilon_0 hc} \cdot F_{BK}(T) + const. \tag{6}$$

$$F_{BK}(T) = \frac{1}{V(T)} \cdot \left[\frac{2n(T)^2+1}{n(T)^2+2} \cdot \left(\frac{\varepsilon(T)-1}{\varepsilon(T)+1} - \frac{n(T)^2-1}{n(T)^2+2}\right) + \frac{3\left(n(T)^4-1\right)}{\left(n(T)^2+2\right)^2}\right] \tag{7}$$

(see Fig. 7)

Table 3 summarizes the ground and excited state dipole moments of 12-DCB and 13-DCB from the LM and BK treatment, described above and compares it to the results of SCS-CC2/cc-pVTZ *ab initio* calculations and to independent experimental determinations of the ground state dipole from microwave Stark spectra [10]. Additionally, the dipole moment of BN has been determined using the above procedure and is compared for the ground and the excited state to the results of electronic Stark spectroscopy from the group of Pratt [8].

5. Discussion

Prior to the discussion of the experimental results and their comparison to the theoretical calculations we have to express a caveat about solvation effects on excited state dipole moments from thermo- or solvatochromic shifts. At first sight it seems plausible to compare gas phase dipole moments from Stark spectroscopy with those from *ab initio* calculations of the isolated species and dipole moments from solvatochromic shifts to *ab initio* calculations which contain solvation effects like the Conductor-like Screening Model (COSMO) or the Polarizable Continuum Model (PCM). This however, is not correct, since the solvent polarity functions defined by Lippert–Mataga, Bilot–Kawski, McRae, Bakhshiev, and Chamma–Viallet, to name only the most popular, establish a correlation between the solvent shifts of fluorescence or absorption transitions and the dipole moment of the **unpolarized** molecule. Hence, the so determined dipole moments will resemble more the results from *ab initio* calculations of the isolated species than of that of solvation models, which return the values of the **polarized** molecule.

Since COSMO is not available for CC2 wave functions, we first assessed the ground state dipole moments of he isolated molecules by MP2 and the excited states dipoles by ADC(2) and compared them to the respective CC2 values, cf. Table 3. All calculations have been performed using Dunning's triple-ζ cc-pVTZ basis set. The close agreement of the dipole moments (as well as rotational constants and excitation energies, etc.) shows that the level of theory is adequate for a calculations of the molecular parameters.

As has been shown previously, the results for excited state dipole moments from application of the original Lippert–Mataga theory are inferior to those from the modified Bilot–Kawski ansatz [24,27,29–31]. For 12-DCB, using BK, we find a value of 6.88 D in the S_1 state, in perfect agreement with the SCS-CC2/cc-pVTZ and the ADC(2)/cc-pVTZ calculated values, while the respective ADC(2) COSMO value for EA as solvent is by 2 Debye too large, cf. Table 3. The value from a evaluation using LM theory is 11.0 D, far from what can be expected.

For 13-DCB, BK theory yields 4.33 D in good agreement with the SCS-CC2 and ADC(2) values of the isolated molecule of 4.11 D, while again the LM value of 8.5 D is about a factor of two too high. As for 12-DCG, the ADC(2) COSMO value is considerably too high (5.27 D). The additivity of bond dipole moments has made the concept of the dipole

Table 3
Dipole moments in Debye obtained from the method of Lippert-Mataga and of Bilot-Kawski compared to those from SCS-CC2/cc-pVTZ calculations for the ground (S_0) and lowest excited singlet states (S_1, S_2), and to independent determinations from evaluation of MW Stark [10] and UV Stark spectra [8].

	BN			12-DCB			13-DCB		
	S_0	S_1	S_2	S_0	S_1	S_2	S_0	S_1	S_2
SCS-CC2	4.43	4.52	4.93	6.95	6.88	7.27	4.18	4.11	4.04
MP2	4.43	–	–	6.98	–	–	4.18	–	–
ADC(2)	–	4.52	5.02	–	6.90	7.29	–	4.11	4.14
MP2 (COSMO)	5.45	–	–	10.04	–	–	5.87	–	–
ADC(2) (COSMO)	–	5.50	5.42	–	8.88	8.63	–	5.27	4.94
Exp.(MW)	4.48[8]	4.57[8]	–	6.82[10]	–	–	3.99[10]	–	–
Exp.(LM)	–	6.8(8)	–	–	11.0(1)	–	–	8.5(2)	–
Exp.(BK)	–	4.42[28]	–	–	6.88(1)	–	–	4.33(3)	–

moment so successful in chemistry. Textbook examples are the isomeric dichloro- and difluorobenzenes in which vector addition allows for a semi-quantitative assessment of the molecular dipole moments from the dipole of the monosubstituted chloro- and fluorobenzenes [3,4]. However, for the excited state of *cis*- and *trans*-3-aminophenol the additivity rule has been shown to yield unsatisfactory results [32].

BN has a ground state dipole moment of 4.48 D [8]. The C-N groups in 12-dicyanobenzene form an angle α of 61.4° [33]. Vectorial addition yields a dipole moment of $\mu_{12} = 2cos(\alpha/2) \cdot \mu = 7.70$ Debye. However, the experimental value is 6.82 Debye [10] (SCS-CC2 calculated: 6.95 D), deviating by 13% from the value obtained by vector addition. For 13-DCB (α=120°) one obtains from vectorial addition a value μ_{13} = 4.48 D, which differs from the experimental value of 3.99 D [10] by 11%. Deviations from vector additivity in the electronic ground state can be attributed to inductive effects on neighboring bonds, which is larger for the neighboring CN groups in 12-DCB.

For the excited state of 12-DCB, the dipole moment from applying BK theory is 6.88 D (SCS-CC2 calculated: 6.88 D), vector addition using the BN excited state dipole of 4.57 D from Ref. [8] yields a value of 7.86 D, which means a deviation of 14% from the experiment. For 13-DCB we obtain 4.33 D from BK theory and 4.57 D from dipole addition (6% deviation).

6. Conclusions

The excited state dipole moments which are obtained from solvatochromic or thermochromic shifts have to be compared to the values of the isolated molecule. These might arise from Stark experiments in the gas phase or in molecular beams or alternatively from *ab initio* calculations. The reason is that solvent shifts of fluorescence or absorption transitions are correlated to the dipole moment of the unpolarized molecule. Keeping this in mind, good agreement is obtained between the calculated and experimentally determined excited state dipole moments.

We were able to show that the deviations of the experimentally determined dipole moments for 12-DCB and 13-DCB from the results of an vector addition in the excited state are similar and in the order of what was found for the electronic ground state. The ground state deviations are similar to those for the textbook example dichlorobenzene. Thus, it is not generally impossible to deduce excited state dipole moments from vector addition of individual dipoles. This is, however, only true for compounds, which have two identical substituents and not for differing substituents like in 3-aminophenol (3AP) [32]. The reduced symmetry in 3-AP leads to a considerable amount of state mixing between the L_a- and L_b-states, which is not present in DCB.

CRediT authorship contribution statement

Matthias Zajonz: Writing – original draft, Software, Methodology, Investigation, Formal analysis. **Tim Oberkirch:** Investigation. **Marie-Luise Hebestreit:** Investigation, Formal analysis. **Mirko Matthias Lindic:** Methodology, Investigation. **Christof Hättig:** Writing – original draft, Formal analysis. **Michael Schmitt:** Writing – original draft, Validation, Supervision, Software, Resources, Project administration, Methodology, Funding acquisition, Conceptualization.

Declaration of competing interest

The authors declare that they have no known competing financial interests or personal relationships that could have appeared to influence the work reported in this paper.

Data availability

Data will be made available on request.

Acknowledgments

Financial support of the Deutsche Forschungsgemeinschaft, Germany via grant SCHM1043/16-1 is gratefully acknowledged. Computational support and infrastructure was provided by the "Center for Information and Media Technology" (ZIM) at the Heinrich-Heine-University Düsseldorf.

Appendix A. Supplementary data

Supplementary material related to this article can be found online at https://doi.org/10.1016/j.jphotochem.2024.115589.

References

[1] P.J.W. Debye, Polare Molekeln, vol. 1, S. Hirzel, Leipzig, 1929,
[2] M. Reinganum, Ann. Phys. 315 (2) (1903) 354–359.
[3] P.W. Atkins, J. de Paula, Atkins' Physical Chemistry, W. H. Freeman and Company New York, New York, 2006.
[4] A. Gossauer, Structure and Reactivity of Biomolecules, Wiley-VHCA, Zürich, 2018.
[5] B.A. McGuire, A.M. Burkhardt, S. Kalenskii, C.N. Shingledecker, A.J. Remijan, E. Herbst, M.C. McCarthy, Science 359 (6372) (2018) 202–205.
[6] O. Chitarra, K.L.K. Lee, Z. Buchanan, M. Melosso, B.A. McGuire, M. Goubet, O. Pirali, M.-A. Martin-Drumel, Astron. Astrophys. 652 (2021) A163.
[7] B.A. McGuire, R.A. Loomis, A.M. Burkhardt, K.L.K. Lee, C.N. Shingledecker, S.B. Charnley, I.R. Cooke, M.A. Cordiner, E. Herbst, S. Kalenskii, M.A. Siebert, E.R. Willis, C. Xue, A.J. Remijan, M.C. McCarthy, Science 371 (6535) (2021) 1265–1269.
[8] D.R. Borst, T.M. Korter, D.W. Pratt, Chem. Phys. Lett. 350 (2001) 485–490.
[9] D.R. Lide Jr., J. Chem. Phys. 22 (1954) 1577–1578.
[10] T. Sato-Toshima, M. Sakiyama, S. Seki, Bull. Chem. Soc. Jpn. 53 (1980) 2762–2767.
[11] TURBOMOLE V7.5.1 2017, a development of University of Karlsruhe and Forschungszentrum Karlsruhe GmbH, 1989–2007, TURBOMOLE GmbH, since 2007; available from http://www.turbomole.com.
[12] R. Ahlrichs, M. Bär, M. Häser, H. Horn, C. Kölmel, Chem. Phys. Lett. 162 (1989) 165–169.
[13] T.H. Dunning Jr., J. Chem. Phys. 90 (1989) 1007–1023.
[14] C. Hättig, F. Weigend, J. Chem. Phys. 113 (2000) 5154–5161.
[15] C. Hättig, A. Köhn, J. Chem. Phys. 117 (2002) 6939–6951.
[16] C. Hättig, J. Chem. Phys. 118 (2002) 7751–7761.
[17] A. Hellweg, S. Grün, C. Hättig, Phys. Chem. Chem. Phys. 10 (2008) 1159–1169.

[18] F. Weigend, M. Häser, Theo. Chem. Acc. 97 (1–4) (1997) 331–340.
[19] A. Klamt, G. Schüürmann, J. Chem. Soc. Perkin Trans. 2 (1993) 799–805.
[20] C. Hättig, Adv. Quant. Chem. 50 (2005) 37–60.
[21] P. Deglmann, F. Furche, R. Ahlrichs, Chem. Phys. Lett. 362 (2002) 511–518.
[22] J.R. Platt, J. Chem. Phys. 17 (1949) 484–495.
[23] E.G. Demissie, E.T. Mengesha, G.W. Woyessa, J. Photochem. Photobiol. A 337 (2017) 184–191.
[24] M.M. Lindic, M. Zajonz, M.-L. Hebestreit, M. Schneider, W.L. Meerts, M. Schmitt, J. Photochem. Photobiol. A 365 (2018) 213–219.
[25] E. Lippert, Z. Naturforsch. 10A (1955) 541.
[26] N. Mataga, Y. Kaifu, M. Koizumi, Bull. Chem. Soc. Jpn 29 (1956) 465.
[27] L. Bilot, A. Kawski, Z. Naturforsch. 17A (1962) 621–627.
[28] A. Kawski, B. Kuklinski, P. Bojarski, Chem. Phys. Lett. 419 (2006) 309–312.
[29] M.M. Lindic, M. Zajonz, M.-L. Hebestreit, M. Schneider, W.L. Meerts, M. Schmitt, Methods X 7 (2020) 101101–1–101101–12.
[30] M.M. Lindic, M. Schmitt, J. Photochem. Photobiol. A 406 (2021) 112984.
[31] M.M. Lindic, T.A. Oberkirch, J. Tatchen, M. Schmitt, J. Photochem. Photobiol. A 419 (2021) 113476.
[32] J.A. Reese, T.V. Nguyen, T.M. Korter, D.W. Pratt, J. Am. Chem. Soc. 126 (2004) 11387–11392.
[33] F.R. Fronczek, Experimental Crystal Structure Determination, CCDC, 2014, 967891.